



# Sonographic Diagnosis of Cervical Lymph Node Metastasis in Patients with Thyroid Cancer and Comparison of European and Korean Guidelines for Stratifying the Risk of Malignant Lymph Node

Sae Rom Chung<sup>1</sup>, Jung Hwan Baek<sup>1</sup>, Yun Hwa Rho<sup>1</sup>, Young Jun Choi<sup>1</sup>, Tae-Yon Sung<sup>2</sup>, Dong Eun Song<sup>3</sup>, Tae Yong Kim<sup>4</sup>, Jeong Hyun Lee<sup>1</sup>

<sup>1</sup>Department of Radiology and Research Institute of Radiology, University of Ulsan College of Medicine, Asan Medical Center, Seoul, Korea; Departments of <sup>2</sup>Surgery, <sup>3</sup>Pathology, and <sup>4</sup>Internal Medicine, University of Ulsan College of Medicine, Asan Medical Center, Seoul, Korea

**Objective:** To evaluate the ultrasonography (US) features for diagnosing metastasis in cervical lymph nodes (LNs) in patients with thyroid cancer and compare the US classification of risk of LN metastasis between European and Korean guidelines.

**Materials and Methods:** From January 2014 to December 2018, US-guided fine-needle aspiration was performed on 836 LNs from 714 patients for the preoperative nodal staging of thyroid cancer. The US features of LNs were retrospectively reviewed for the following features: size, presence of hilum, margin, orientation, cystic change, punctate echogenic foci (PEF), large echogenic foci, eccentric cortical thickening, abnormal vascularity, and cortical hyperechogenicity. A multiple logistic regression analysis was performed to identify the independent US features for the diagnosis of metastatic LNs. The diagnostic performance of independent US features was subsequently evaluated. LNs were categorized according to the Korean Thyroid Imaging Reporting and Data System (K-TIRADS) and European Thyroid Association (ETA) guidelines, and the correlation between the two sets of classifications was assessed.

**Results:** Absence of the hilum, presence of cystic changes, PEF, abnormal vascularity, and cortical hyperechogenicity were independent US features of metastatic LNs. Cystic changes, PEF, abnormal vascularity, and cortical hyperechogenicity showed high specificity (86.8%–99.6%). The absence of the hilum had the highest sensitivity yet low specificity (66.4%). When LNs were classified according to the ETA guidelines and K-TIRADS, they yielded similar categorizations of malignancy risks and were strongly correlated (Spearman coefficient, 0.9766 [95% confidence interval, 0.973–0.979]). According to the ETA guidelines, 9.8% (82/836) of LNs were classified as “not specified.”

**Conclusion:** Absence of hilum, cystic changes, PEF, abnormal vascularity, and cortical hyperechogenicity were independent US features suggestive of metastatic LNs in thyroid cancer. Both K-TIRADS and the ETA guidelines provided similar risk stratification for metastatic LNs with a high correlation; however, the ETA guidelines failed to classify 9.8% of LNs into a specific risk stratum. These results may provide a basis for revising LN classification in future guidelines.

**Keywords:** Thyroid; Thyroid cancer; Lymph node; Ultrasonography; Metastasis

## INTRODUCTION

Differentiated thyroid carcinoma (DTC) is the most common malignant thyroid tumor, with an excellent

prognosis [1]. However, DTCs manifest as regional lymph node (LN) metastases at the time of diagnosis in 30%–80% of cases [2–5]. The accurate preoperative diagnosis of LN metastasis is important for patients with DTCs to

**Received:** April 16, 2021 **Revised:** August 11, 2022 **Accepted:** August 18, 2022

**Corresponding author:** Jung Hwan Baek, MD, PhD, Department of Radiology and Research Institute of Radiology, University of Ulsan College of Medicine, Asan Medical Center, 88 Olympic-ro 43-gil, Songpa-gu, Seoul 05505, Korea.

• E-mail: radbaek@naver.com

This is an Open Access article distributed under the terms of the Creative Commons Attribution Non-Commercial License (<https://creativecommons.org/licenses/by-nc/4.0>) which permits unrestricted non-commercial use, distribution, and reproduction in any medium, provided the original work is properly cited.

determine the optimal surgical extent and reduce persistent or recurrent disease and reoperation complications [6]. Moreover, LN metastasis is an important prognostic factor; particularly, lateral LN metastasis increases the risk of locoregional recurrence and decreases the rate of disease-free survival among patients with papillary thyroid carcinoma [1,4,7,8].

Ultrasonography (US) is the most sensitive method for the detection of metastatic LNs. Several US features have been used to differentiate metastatic LNs from benign LNs, including size enlargement, absence of fatty hilum, round shape, hyperechoic cortical change, calcification, cystic change, and abnormal vascularity on Doppler imaging [9-16]. Recently, several guidelines for thyroid cancer have defined suspicious LNs in the assessment of DTC [17-19]. The Korean Thyroid Imaging Reporting and Data System (K-TIRADS), proposed by the Korean Society of Thyroid Radiology/Korean Thyroid Association, and the European Thyroid Association (ETA) guidelines for cervical US scans have categorized LNs into three groups. However, the US features corresponding to each category are not the same between K-TIRADS and the ETA guidelines, and the diagnostic performance of US features suggestive of metastatic LNs from DTC shows different results between studies [9,10,13,20-22]. Thus, this study aimed to evaluate the US features for diagnosing metastasis in cervical LNs in patients with thyroid cancer and compare the classification of risk of LN metastasis between the current ETA guidelines and K-TRADS.

## MATERIALS AND METHODS

This retrospective study was approved by the Institutional Review Board of our institution. The requirement for informed consent was waived owing to the retrospective nature of the analyses and use of anonymized medical records. Methods and data reporting were performed in accordance with the Standards for Reporting of Diagnostic Accuracy Studies [23].

### Patient Selection

Consecutive patients with DTC who underwent US-guided fine needle aspiration (FNA) of the LNs at our institution between January 2014 and December 2018 were included. Patients were included if they met the following criteria: 1) underwent FNA for preoperative evaluation and 2) had a final diagnosis of DTC for thyroid cancer. Patients were excluded if they had undergone FNA of the LNs for persistent

or recurrent disease after surgery for thyroid cancer or if they had not undergone subsequent surgical resection or follow-up imaging for at least 1 year. Finally, 836 LNs from 714 patients were included in this study (Fig. 1).

### US and US-FNA

Thyroid US examination was performed using an iU22 or HDI-5000 unit (Philips Healthcare) or an EUB-7500 unit (Hitachi Medical Systems) with a 5–14-MHz linear high-frequency probe. All US examinations and US-guided FNAs were performed by radiologists under the supervision of staff radiologists with > 14 years of clinical experience in evaluating thyroid US images. Radiologists classified LNs into benign, indeterminate, and suspicious according to the 2016 K-TIRADS [24]. Radiologists performed US-guided FNA of an indeterminate or suspicious LN when it may affect the surgical extent of thyroid cancer, regardless of their size. Sonographically benign LNs were examined at the clinician's discretion. When there are multiple suspicious LNs in one compartment, an easily accessible LN is selected for FNA.

### Imaging Analysis

US images were evaluated independently by two radiologists with 11 and 5 years of experience in thyroid US imaging, respectively, who were unaware of the patients' clinical histories, previous imaging results, or cytopathology results. Any disagreements after independent interpretations were resolved by discussion, and consensus results were used for the main study analysis.

The US findings of the LNs were evaluated for the following features: location (levels I–VI), size, presence of hilum, margin (smooth or irregular), orientation (parallel or nonparallel), presence of cystic change,

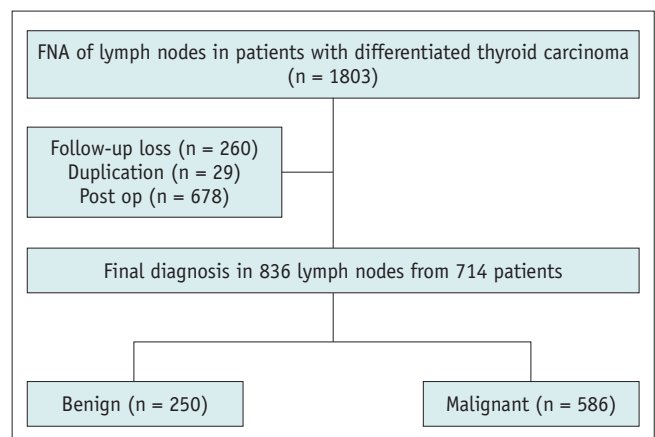


**Fig. 1. Flow chart of the study population.** FNA = fine needle aspiration

punctate echogenic foci (PEF, echogenic foci  $\leq 1$  mm), large echogenic foci ( $> 1$  mm), eccentric cortical thickening, abnormal vascularity (peripheral or diffuse), and cortical hyperechogenicity. For size measurement, the short and long diameters were both measured in the most representative longitudinal nodal plane showing the LN maximum and minimum diameters, and the long-to-short diameter (L/S) ratio was calculated. For LNs with a hilum, the presence of eccentric cortical thickening was evaluated. LNs in which the cortex does not show a uniform thickness around the hilum and are thickened focally at least twice the narrowest point of the cortex were classified as having eccentric cortical thickening [25]. Cortical hyperechogenicity was assessed using a reference structure of the anterior neck muscles (strap or sternocleidomastoid muscles).

### Classification of LNs

US features were used to stratify the risk of malignancy of LNs into three categories of the K-TIRADS and ETA guidelines (probably benign, indeterminate, and suspicious in K-TIRADS and normal, indeterminate, and suspicious for malignancy in the ETA guidelines) (Supplementary Table 1). LNs were classified as “not specified” by the ETA guidelines if they satisfied at least one of the following criteria: 1) presence of normal hilum and round shape, 2) presence of normal hilum and increased size (short axis  $\geq 8$  mm in level II and  $\geq 5$  mm in levels III and IV), or 3) absence of normal hilum, oval shape, and normal size.

### Reference Standard

LNs were finally diagnosed as metastatic if they showed malignant FNA cytology and/or elevated washout thyroglobulin (Tg) ( $> 8.3$  ng/mL) [26]. Considering the false positivity of washout Tg, in case of increased washout Tg levels with benign or insufficient cytological results, the patient was diagnosed with metastatic LN by repeat biopsy or surgical resection. LNs with benign or indeterminate FNA cytology and normal washout Tg were finally diagnosed as benign if they satisfied at least one of the following criteria: 1) confirmation based on the surgical specimen, 2) subsequent repeat FNA or core-needle biopsy, and 3) decreased size on follow-up imaging after more than 1 year.

### Statistical Analysis

To compare the clinicoradiological features between metastatic and benign LNs, a *t* test was used for continuous variables, and the chi-square or Fisher's exact test was

used for categorical variables. A multivariable logistic regression analysis following a series of univariable analyses was used to identify independent US features associated with metastatic LNs in patients with thyroid cancer. univariable and multivariable analyses were based on generalized estimating equations with a logit link function to account for data clustering. The diagnostic performance of US features that showed a significant independent association with metastatic LNs for diagnosing metastatic LN was subsequently evaluated in terms of sensitivity, specificity, positive and negative predictive values, and diagnostic accuracy. Interobserver agreement between the two radiologists was calculated using Cohen's kappa statistic. Values less than 0.20 were considered indicative of slight agreement, 0.21–0.40 indicative of fair agreement, 0.41–0.60 indicative of moderate agreement, 0.61–0.80 indicative of substantial agreement, and 0.81–1.00 indicative of near-perfect agreement.

The K-TIRADS and ETA guidelines were applied to the US findings, and the estimated malignancy rates were calculated for each guideline category. Correlations between K-TIRADS (1, 2, and 3 for probably benign, indeterminate, and suspicious categories, respectively) and the ETA (1, 2, 3, and 4 for normal, indeterminate, suspicious for malignancy, and not specified, respectively) guidelines were analyzed using Spearman's rank correlation coefficients.

All statistical analyses were performed using SAS version 9.4 (SAS Institute) and MedCalc version 19.1 (MedCalc Software). All tests were two-sided, and a *p* value  $< 0.05$  was considered statistically significant.

## RESULTS

### Study Population

A total of 836 LNs from 717 patients were included in this study. Of the 836 LNs, 250 (29.9%) were benign, and 586 (70.1%) were metastatic, including 573 with papillary thyroid carcinoma, 12 with follicular variant papillary thyroid carcinoma, and 1 with follicular carcinoma. A total of 250 benign LNs were confirmed by additional biopsy ( $n = 11$ ), a decrease in size on serial follow-up US imaging ( $n = 227$ ), or surgical resection ( $n = 12$ ). The preoperative serum Tg were measured in 285 patients, and there was no significant difference in the mean serum Tg level between benign and metastatic LNs ( $34.68 \pm 68.15$  ng/mL for benign LNs and  $68.39 \pm 315.82$  ng/mL for metastatic LNs,  $p = 0.171$ ).

**US Features for Diagnosing Metastatic LNs from Thyroid Cancer**

Table 1 lists the clinical and US features of benign and metastatic LNs. Metastatic LNs were significantly associated with male sex (38.2% vs. 24%,  $p < 0.001$ ). Among the US features, the size of LNs and L/S ratio, irregular margin, non-parallel orientation, eccentric cortical thickening, absence of hilum, presence of cystic change, PEF, peripheral vascularity, and cortical hyperechogenicity were associated with metastatic LNs. Large echogenic foci within LNs were more common in metastatic LNs; however, this difference was not significant (3.2% vs. 6.5%,  $p = 0.057$ ). The results of the multivariable logistic regression analyses to determine the independent US features associated with metastatic LNs from the thyroid are listed in Table 2. The US features of the absence of hilum,

presence of cystic changes, PEF, abnormal vascularity, and cortical hyperechogenicity were independently significantly associated with metastatic LNs (Figs. 2-4).

**Table 2. Results of Multivariable Logistic Regression Analysis of the Association between US Features and Metastatic Lymph Nodes**

| US Features                | Adjusted OR | 95% Confidence Interval | P       |
|----------------------------|-------------|-------------------------|---------|
| Absence of hilum           | 2.407       | 2.056–2.758             | < 0.001 |
| Cystic changes             | 84.259      | 10.034–707.544          | < 0.001 |
| Punctate echogenic foci    | 3.105       | 1.810–5.325             | < 0.001 |
| Abnormal vascularity       | 5.860       | 2.976–11.537            | < 0.001 |
| Cortical hyperechogenicity | 7.907       | 4.495–13.908            | < 0.001 |

OR = odds ratio, US = ultrasonography

**Table 1. Summary of Demographic and Ultrasonography Features**

| Characteristics               | Benign (n = 250) | Metastatic (n = 586) | Malignancy Rate (%) | P       |
|-------------------------------|------------------|----------------------|---------------------|---------|
| Sex                           |                  |                      |                     | < 0.001 |
| Male                          | 60 (24.0)        | 224 (38.2)           |                     |         |
| Female                        | 190 (76.0)       | 362 (61.8)           |                     |         |
| Age, year*                    | 47.86 ± 12.85    | 47.53 ± 14.21        |                     | 0.063   |
| Location                      |                  |                      |                     | 0.051   |
| Level II                      | 25 (10.0)        | 48 (8.2)             |                     |         |
| Level III                     | 70 (28.0)        | 214 (36.5)           |                     |         |
| Level IV                      | 144 (57.6)       | 306 (52.2)           |                     |         |
| Level V                       | 5 (2.0)          | 3 (0.5)              |                     |         |
| Level VI                      | 6 (2.4)          | 15 (2.5)             |                     |         |
| Short diameter, cm*           | 0.419 ± 0.16     | 0.603 ± 0.39         |                     | < 0.001 |
| Long diameter, cm*            | 1.144 ± 0.56     | 1.197 ± 0.67         |                     | 0.001   |
| Size enlargement              | 62 (24.8)        | 284 (48.5)           | 82.1                | < 0.001 |
| L/S ratio < 1.5               | 24 (9.6)         | 140 (23.9)           | 85.4                | < 0.001 |
| L/S ratio < 2                 | 74 (29.6)        | 308 (52.6)           | 80.6                | < 0.001 |
| Margin                        |                  |                      |                     | < 0.001 |
| Smooth                        | 180 (72.0)       | 173 (29.5)           | 49.0                |         |
| Irregular                     | 70 (28.0)        | 413 (70.5)           | 85.5                |         |
| Orientation                   |                  |                      |                     | 0.049   |
| Parallel                      | 240 (96.0)       | 541 (92.3)           | 69.3                |         |
| Nonparallel                   | 10 (4.0)         | 45 (7.7)             | 81.8                |         |
| Eccentric cortical thickening | 48 (28.9)        | 50 (8.8)             | 33.9                | < 0.001 |
| Hilum                         |                  |                      |                     | < 0.001 |
| Absent                        | 84 (33.6)        | 501 (85.5)           | 85.6                |         |
| Present                       | 166 (66.4)       | 85 (14.5)            | 33.9                |         |
| Cystic changes                | 1 (0.4)          | 151 (25.8)           | 99.3                | < 0.001 |
| Punctate echogenic foci       | 33 (13.2)        | 304 (51.9)           | 90.2                | < 0.001 |
| Large echogenic foci          | 8 (3.2)          | 38 (6.5)             | 82.6                | 0.057   |
| Abnormal vascularity          | 15 (6.0)         | 386 (65.9)           | 96.4                | < 0.001 |
| Cortical hyperechogenicity    | 33 (13.2)        | 491 (83.8)           | 93.7                | < 0.001 |

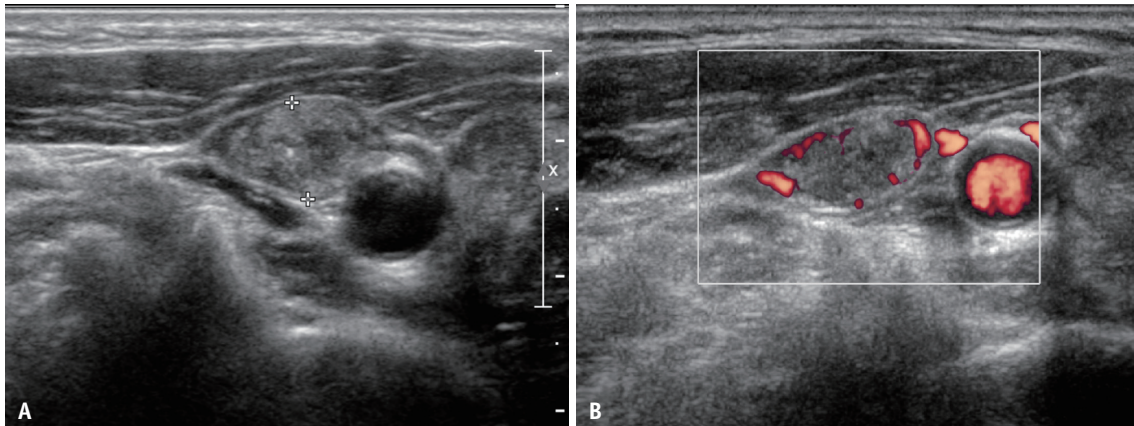
Data are expressed as the number of cases with percentages in parentheses unless otherwise indicated. \*Data are expressed as mean ± standard deviation. L/S ratio = long-to-short diameter ratio



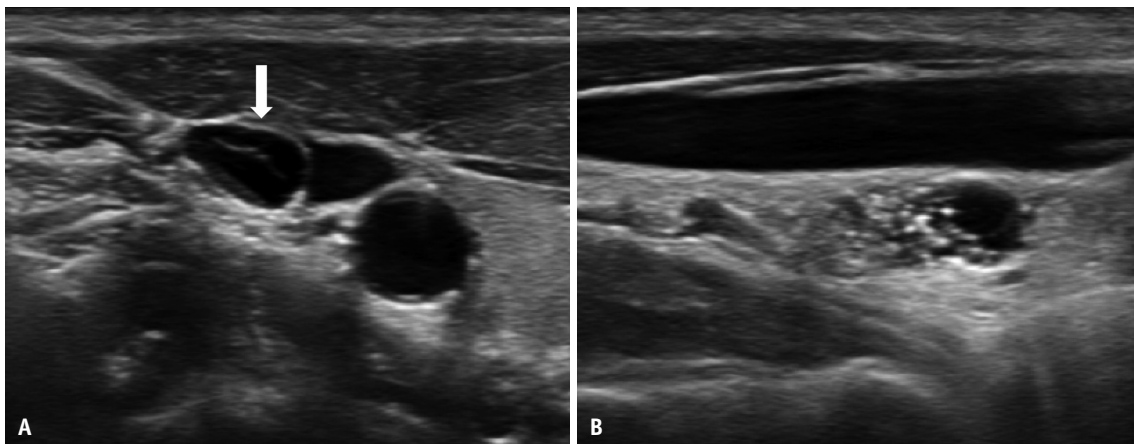
**Diagnostic Performance of Each US Feature for the Depiction of Metastatic LNs**

Table 3 presents the diagnostic performance of the US

features of LNs suggestive of metastasis. Although absence of the hilum showed a relatively high sensitivity (85.5%), it was limited by a relatively low specificity (66.4%). In



**Fig. 2.** Transverse ultrasonography images of metastatic lymph nodes in a 65-year-old female showing diffuse hyperechogenicity with punctate echogenic foci without demonstrable normal hilar structure (A). Doppler study reveals increased vascularity in the peripheral of the lymph node (B).



**Fig. 3.** Transverse (A) and longitudinal (B) ultrasonography images of the metastatic lymph node in a 41-year-old female showing intranodal cystic changes (arrow) with cortical hyperechogenicity and punctate echogenic foci.

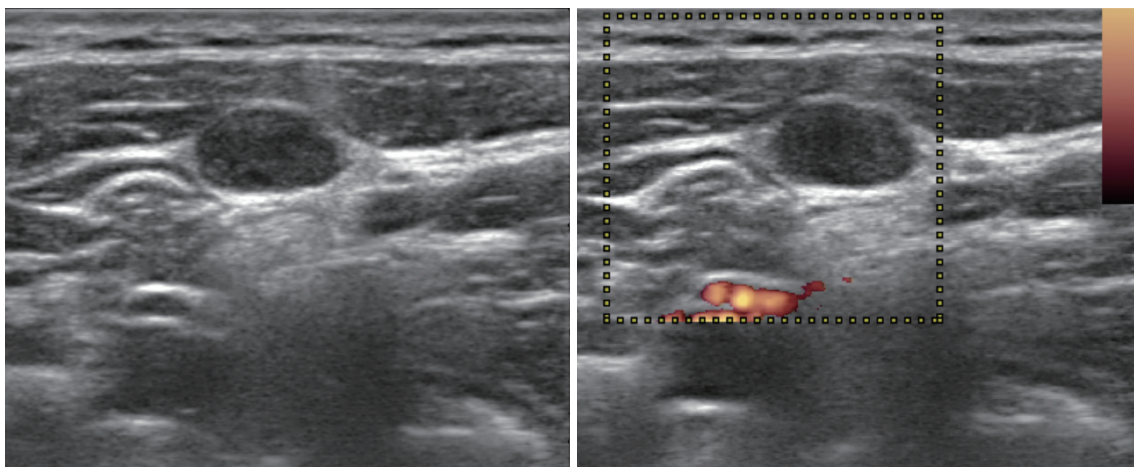


**Fig. 4.** Transverse ultrasonography image of metastatic lymph nodes in a 36-year-old female showing no demonstrable echogenic hilum or hilar vascularity. Cortical echogenicity is similar to that of the anterior neck muscle.

**Table 3. Diagnostic Accuracy of US Findings for Metastatic Lymph Nodes**

| US Features                | Sensitivity    | Specificity    | PPV            | NPV            | Accuracy       |
|----------------------------|----------------|----------------|----------------|----------------|----------------|
| Absence of hilum           | 85.5 (501/586) | 66.4 (166/250) | 85.6 (501/585) | 66.1 (166/251) | 79.8 (667/836) |
| Cystic changes             | 25.8 (151/586) | 99.6 (249/250) | 99.3 (151/152) | 36.4 (249/684) | 47.8 (400/836) |
| Punctate echogenic foci    | 51.9 (304/586) | 86.8 (217/250) | 90.2 (304/337) | 43.5 (217/499) | 62.3 (521/836) |
| Abnormal vascularity       | 67.7 (397/586) | 94.0 (235/250) | 96.4 (397/412) | 55.4 (235/424) | 75.6 (632/836) |
| Cortical hyperechogenicity | 83.8 (491/586) | 86.8 (217/250) | 93.7 (491/524) | 69.6 (217/312) | 84.7 (708/836) |

Data are % with the raw number of nodules in parentheses. NPV = negative predictive value, PPV = positive predictive value, US = ultrasonography

contrast, the other features, namely cystic change, PEF, abnormal vascularity, and cortical hyperechogenicity, showed high specificities (86.8%–99.6%). However, the sensitivity was relatively low (25.8%–67.7%) for cystic changes, PEF, and abnormal vascularity. Cortical hyperechogenicity showed relatively high sensitivity (83.8%) and the highest diagnostic accuracy (84.7%).

#### Interobserver Agreement of Sonographic Features

The interobserver agreement on sonographic features is summarized in Table 4. Between readers 1 and 2, the strength of agreement ranged from fair to substantial (kappa value [ $\kappa$ ] range, 0.224–0.654). PEF and abnormal vascularity showed substantial interobserver agreement ( $\kappa = 0.654$  and  $\kappa = 0.609$ , respectively). Eccentric cortical thickening and irregular margins showed fair interobserver agreement ( $\kappa = 0.224$  and  $\kappa = 0.331$ , respectively). Other features, including echogenic hilum or hilar vascularity, large echogenic foci, cystic changes, and cortical hyperechogenicity, showed fair agreement.

#### LN Classification according to the ETA Guidelines and K-TIRADS

The classification of LNs according to the ETA guidelines and K-TIRADS and the malignancy rate of each category are shown in Table 5. The overall malignancy risks for the normal, indeterminate, and suspicious malignancy categories of the ETA guidelines were 13.8%, 28.3%, and 90.0%, respectively, while those for the probably benign, indeterminate, and suspicious categories of the K-TIRADS were 13.4%, 29.9%, and 90.0%, respectively. In the assessment of ETA categories, 82 of 836 LNs (9.8%) did not meet the criteria for any pattern and were thus classified as “not specified.” The malignancy risk of LNs classified as “not specified” was 19.5% (16/82 LNs). The correlation coefficient between the categorizations according to the K-TIRADS and ETA guidelines was 0.9766 (95% confidence interval, 0.973–0.979;  $p < 0.001$ ).

**Table 4. Inter-Observer Agreement of Sonographic Features**

| Sonographic Features          | Kappa | 95% Confidence Interval |
|-------------------------------|-------|-------------------------|
| Eccentric cortical thickening | 0.224 | 0.144–0.304             |
| Echogenic hilum               | 0.524 | 0.461–0.588             |
| Hilar vascularity             | 0.509 | 0.445–0.574             |
| Irregular margin              | 0.331 | 0.272–0.389             |
| Nonparallel orientation       | 0.461 | 0.354–0.568             |
| Punctate echogenic foci       | 0.654 | 0.602–0.706             |
| Large echogenic foci          | 0.477 | 0.356–0.598             |
| Abnormal vascularity          | 0.609 | 0.556–0.662             |
| Cortical hyperechogenicity    | 0.467 | 0.409–0.523             |
| Cystic change                 | 0.453 | 0.369–0.536             |

**Table 5. Malignancy Rate of Lymph Nodes Classified according to the K-TIRADS and ETA Guidelines**

|                           | No. of Cases | Metastatic Lymph Nodes | Malignancy Rate (%) |
|---------------------------|--------------|------------------------|---------------------|
| ETA guideline category    |              |                        |                     |
| Normal                    | 109          | 15                     | 13.8                |
| Indeterminate             | 46           | 13                     | 28.3                |
| Suspicious for malignancy | 599          | 542                    | 90.0                |
| Not specified             | 82           | 16                     | 19.5                |
| K-TIRADS category         |              |                        |                     |
| Probably benign           | 157          | 21                     | 13.4                |
| Indeterminate             | 77           | 23                     | 29.9                |
| Suspicious                | 602          | 542                    | 90.0                |

ETA = European Thyroid Association, K-TIRADS = Korean Thyroid Imaging Reporting and Data System

## DISCUSSION

Our study demonstrated that the absence of hilum, presence of cystic changes, PEF, abnormal vascularity, and cortical hyperechogenicity were independent US features differentiating metastatic LNs from benign LNs in thyroid cancer at preoperative evaluation. Cystic change, PEF, abnormal vascularity, and cortical hyperechogenicity showed high specificities (86.8%–99.6%). The absence of hilum

had the highest sensitivity; however, the specificity was low (66.4%). When LNs were classified according to K-TIRADS and the ETA guidelines, the corresponding categories of the two guidelines showed similar malignancy rates with a high correlation between both guidelines. However, the ETA guidelines failed to categorize LNs into a specific risk stratum in 9.8% of LNs.

Several US features have been proposed to differentiate metastatic LNs from benign LNs in thyroid cancer, including size enlargement, absence of fatty hilum, round shape, nonparallel orientation, eccentric cortical thickening, hyperechoic cortical change, calcification, cystic change, and abnormal vascularity on Doppler imaging [11,16,21]. Among these, five US features, namely hilum absence, presence of cystic changes, PEF, abnormal vascularity, and cortical hyperechogenicity, were independently associated with metastatic LNs. Our study results differed from those of Yoo et al. [21], which showed that eccentric cortical thickening and cortical hyperechogenicity were significantly associated with metastatic LNs. This is possibly due to the difference in the study population (central LN vs. all LNs) and the imaging analysis method. In our study, eccentric cortical thickening was analyzed only in LNs with the hilum, according to a previous study [25]. Lee et al. [27] reported similar results in that the presence of cystic changes, EF, abnormal vascularity, and cortical hyperechogenicity were independently associated with metastatic LNs. However, contrary to the results of our study, the absence of a hilum was not revealed as an independent factor suggesting metastatic LNs. This is probably because we analyzed a larger patient group in our study (836 vs. 346). Moreover, our study analyzed the interobserver agreement for US features suggestive of metastatic LNs in patients with thyroid cancer, and, to our knowledge, such results have not been previously reported. All five US features independently associated with metastatic LNs showed moderate to substantial agreement (0.467–0.654).

Among the five significant US features, four showed very high specificity: presence of cystic changes, PEF, abnormal vascularity, and cortical hyperechogenicity. Particularly, cystic changes showed high specificity (99.6%). This is consistent with previous studies reporting 100% specificity for cystic changes [9,11,21,22]. In our study, one patient with cystic changes, identified as benign LNs, was diagnosed with tuberculosis. Although the sensitivity of cystic changes was as low as 25%, this feature showed a very high specificity for diagnosing metastatic LNs

from DTC. The diagnostic performance of each US feature reported in our study was within the range reported in previous studies: hilum absence (sensitivity, 31.6%–100%; specificity, 18.6%–92.4%), cystic changes (sensitivity, 11.0%–34.0%; specificity, 87.7%–100%), calcification (sensitivity, 10.0%–49.5%; specificity, 93.0%–100%), abnormal vascularity (sensitivity, 32.7%–86.0%; specificity, 57.1%–97.0%), and cortical hyperechogenicity (sensitivity, 53.1%–86.0%; specificity, 42.9%–95.9%) [9,11,16,21,22]. The sensitivity calculated for PEF was slightly higher than that in previous reports (51.9%), possibly due to the higher-resolution imaging of US used today. The absence of hilum showed the most diverse range of diagnostic performances in previous studies.

Other findings such as size, L/S ratio, irregular margin, and nonparallel orientation were different in the univariable analysis, yet there was no significant difference in the multivariable analysis. Regarding size, we analyzed all variables, including short and long diameter, size enlargement (short axis  $\geq 8$  mm in level II and  $\geq 5$  mm in levels III and IV), and L/S ratio ( $< 1.5$  or  $2.0$ ), and did not find significant results in the multivariable analysis.

Among the various thyroid nodule-related guidelines currently available, only K-TIRADS and EU-TIRADS categorize LNs into three categories: normal, indeterminate, and suspicious for malignancy in the ETA guidelines and probably benign, indeterminate, and suspicious in K-TIRADS. Both the ETA guidelines and K-TIRADS provide effective malignancy risk stratification with a high correlation. However, the US features corresponding to each category were different. For normal (probably benign according to K-TIRADS) and indeterminate categories, both K-TIRADS and the ETA guidelines are defined as having no suspicious features and classified according to the presence or absence of hilum. However, the ETA guidelines also consider shape (round or ovoid) and size [19]. These factors render the ETA guidelines complex, making them less useful in clinical practice, and 9.8% of LNs were “not specified.” According to our study, shape (assessed by L/S ratio) and size did not show a significant relationship with malignancy, and the ETA guidelines had a high correlation with the malignancy rate according to K-TIRADS, which does not consider size and shape. Therefore, when defining benign and indeterminate LNs, the shape and size can be excluded. With this taken into consideration, 82 cases classified as “not specified” according to the ETA guidelines can also be included in the classification.



The definition of US features corresponding to the suspicious for malignancy category (suspicious in K-TIRADS) is almost identical, although K-TIRADS includes large EF and PEF as suspicious US features. In our study, although a large EF was more common in metastatic LNs than in benign LNs, the difference was not significant. This is consistent with the findings of a previous study [21]. Macrocalcifications in LN are a marker of nodal disease, regardless of whether they are benign or malignant. Among benign causes, macrocalcifications most often result from prior granulomatous infections, especially tuberculosis and histoplasmosis. Other, less common causes include sarcoidosis, silicosis, and amyloidosis [28,29]. Although the prevalence of a large EF was low in this study and showed no significant association with that of metastatic LNs in patients with thyroid cancer, the malignancy rate was as high as 82.6%. Thus, LNs with a large EF should be considered as pathologic LNs and require biopsy to exclude metastatic LNs in patients without an evident history of granulomatous infections such as tuberculosis.

Our study has several limitations. First, the evaluation of cases was retrospective, all patients were recruited at a single tertiary referral center, and FNA was not performed for all LNs, leading to an unavoidable bias for selecting LNs for FNA. The high prevalence of metastatic LNs in the study population may have overestimated the malignancy risk for each US predictor. This may be related to the relatively high malignancy rate of LNs that were categorized as benign in our study. Furthermore, there may have been interobserver in the interpretation of the US features of LNs. Thus, prospective multicenter studies are required to validate the generalizability of our findings.

In conclusion, this study identified the absence of hilum, presence of cystic changes, PEF, abnormal vascularity, and cortical hyperechogenicity as independent US features that could discriminate between metastatic and benign LNs. Both K-TIRADS and the ETA guidelines provided similarly effective risk stratification for metastatic LNs with a high correlation. However, the ETA guidelines failed to classify 9.8% of the LNs into a specific risk stratum. Our research results may provide a basis for revising the LN classification in future guidelines.

## Supplement

The Supplement is available with this article at <https://doi.org/10.3348/kjr.2022.0358>.

## Availability of Data and Material

The datasets generated or analyzed during the study are available from the corresponding author on reasonable request.

## Conflicts of Interest

Jung Hwan Baek and Jeong Hyun Lee who is on the editorial board of the *Korean Journal of Radiology* was not involved in the editorial evaluation or decision to publish this article. Financial activities not related to the present article. Consultant of two radiofrequency companies, STARmed and RF medical since 2017. All remaining authors have declared no conflicts of interest.

## Author Contributions

Conceptualization: Jung Hwan Baek, Sae Rom Chung. Data curation: Sae Rom Chung. Formal analysis: Sae Rom Chung. Investigation: Sae Rom Chung, Yun Hwa Rho, Jung Hwan Baek. Methodology: Sae Rom Chung, Tae Yong Kim, Tae-Yon Sung, Dong Eun Song. Project administration: Sae Rom Chung. Supervision: Jung Hwan Baek. Validation: Yun Hwa Rho. Visualization: Sae Rom Chung. Writing—original draft: Sae Rom Chung. Writing—review & editing: Jung Hwan Baek, Young Jun Choi, Jeong Hyun Lee.

## ORCID iDs

Sae Rom Chung

<https://orcid.org/0000-0003-4219-7166>

Jung Hwan Baek

<https://orcid.org/0000-0003-0480-4754>

Yun Hwa Rho

<https://orcid.org/0000-0002-8041-1621>

Young Jun Choi

<https://orcid.org/0000-0001-7098-5042>

Tae-Yon Sung

<https://orcid.org/0000-0002-2179-6269>

Dong Eun Song

<https://orcid.org/0000-0002-9583-9794>

Tae Yong Kim

<https://orcid.org/0000-0003-4982-4441>

Jeong Hyun Lee

<https://orcid.org/0000-0002-0021-4477>

## Funding Statement

None



## REFERENCES

1. Arianpoor A, Asadi M, Amini E, Ziaemehr A, Ahmadi Simab S, Zakavi SR. Investigating the prevalence of risk factors of papillary thyroid carcinoma recurrence and disease-free survival after thyroidectomy and central neck dissection in Iranian patients. *Acta Chir Belg* 2020;120:173-178
2. King JM, Corbitt C, Miller FR. Management of lateral cervical metastases in papillary thyroid cancer: patterns of lymph node distribution. *Ear Nose Throat J* 2011;90:386-389
3. Shaha AR. Management of the neck in thyroid cancer. *Otolaryngol Clin North Am* 1998;31:823-831
4. Roh JL, Kim JM, Park CI. Lateral cervical lymph node metastases from papillary thyroid carcinoma: pattern of nodal metastases and optimal strategy for neck dissection. *Ann Surg Oncol* 2008;15:1177-1182
5. McGregor GI, Luoma A, Jackson SM. Lymph node metastases from well-differentiated thyroid cancer. A clinical review. *Am J Surg* 1985;149:610-612
6. Watkinson JC, Franklyn JA, Olliff JF. Detection and surgical treatment of cervical lymph nodes in differentiated thyroid cancer. *Thyroid* 2006;16:187-194
7. Ito Y, Kudo T, Kobayashi K, Miya A, Ichihara K, Miyauchi A. Prognostic factors for recurrence of papillary thyroid carcinoma in the lymph nodes, lung, and bone: analysis of 5,768 patients with average 10-year follow-up. *World J Surg* 2012;36:1274-1278
8. Ywata de Carvalho A, Kohler HF, Gomes CC, Vartanian JG, Kowalski LP. Predictive factors for recurrence of papillary thyroid carcinoma: analysis of 4,085 patients. *Acta Otorhinolaryngol Ital* 2021;41:236-242
9. Rosário PW, de Faria S, Bicalho L, Alves MF, Borges MA, Purisch S, et al. Ultrasonographic differentiation between metastatic and benign lymph nodes in patients with papillary thyroid carcinoma. *J Ultrasound Med* 2005;24:1385-1389
10. Kuna SK, Bracic I, Tesic V, Kuna K, Herceg GH, Dodig D. Ultrasonographic differentiation of benign from malignant neck lymphadenopathy in thyroid cancer. *J Ultrasound Med* 2006;25:1531-1537; quiz 1538-1540
11. Jeon SJ, Kim E, Park JS, Son KR, Baek JH, Kim YS, et al. Diagnostic benefit of thyroglobulin measurement in fine-needle aspiration for diagnosing metastatic cervical lymph nodes from papillary thyroid cancer: correlations with US features. *Korean J Radiol* 2009;10:106-111
12. Miseikyte-Kaubriene E, Trakymas M, Ulys A. Cystic lymph node metastasis in papillary thyroid carcinoma. *Medicina (Kaunas)* 2008;44:455-459
13. Fish SA, Langer JE, Mandel SJ. Sonographic imaging of thyroid nodules and cervical lymph nodes. *Endocrinol Metab Clin North Am* 2008;37:401-417, ix
14. Kessler A, Rappaport Y, Blank A, Marmor S, Weiss J, Graif M. Cystic appearance of cervical lymph nodes is characteristic of metastatic papillary thyroid carcinoma. *J Clin Ultrasound* 2003;31:21-25
15. Wunderbaldinger P, Harisinghani MG, Hahn PF, Daniels GH, Turetschek K, Simeone J, et al. Cystic lymph node metastases in papillary thyroid carcinoma. *AJR Am J Roentgenol* 2002;178:693-697
16. Sohn YM, Kwak JY, Kim EK, Moon HJ, Kim SJ, Kim MJ. Diagnostic approach for evaluation of lymph node metastasis from thyroid cancer using ultrasound and fine-needle aspiration biopsy. *AJR Am J Roentgenol* 2010;194:38-43
17. Haugen BR, Alexander EK, Bible KC, Doherty GM, Mandel SJ, Nikiforov YE, et al. 2015 American Thyroid Association management guidelines for adult patients with thyroid nodules and differentiated thyroid cancer: the American Thyroid Association guidelines task force on thyroid nodules and differentiated thyroid cancer. *Thyroid* 2016;26:1-133
18. Ha EJ, Chung SR, Na DG, Ahn HS, Chung J, Lee JY, et al. 2021 Korean thyroid imaging reporting and data system and imaging-based management of thyroid nodules: Korean Society of Thyroid Radiology consensus statement and recommendations. *Korean J Radiol* 2021;22:2094-2123
19. Leenhardt L, Erdogan MF, Hegedus L, Mandel SJ, Paschke R, Rago T, et al. 2013 European thyroid association guidelines for cervical ultrasound scan and ultrasound-guided techniques in the postoperative management of patients with thyroid cancer. *Eur Thyroid J* 2013;2:147-159
20. Kim DW, Choo HJ, Lee YJ, Jung SJ, Eom JW, Ha TK. Sonographic features of cervical lymph nodes after thyroidectomy for papillary thyroid carcinoma. *J Ultrasound Med* 2013;32:1173-1180
21. Yoo YH, Kim JA, Son EJ, Youk JH, Kwak JY, Kim EK, et al. Sonographic findings predictive of central lymph node metastasis in patients with papillary thyroid carcinoma: influence of associated chronic lymphocytic thyroiditis on the diagnostic performance of sonography. *J Ultrasound Med* 2013;32:2145-2151
22. Leboulleux S, Girard E, Rose M, Travaglini JP, Sabbah N, Caillou B, et al. Ultrasound criteria of malignancy for cervical lymph nodes in patients followed up for differentiated thyroid cancer. *J Clin Endocrinol Metab* 2007;92:3590-3594
23. Cohen JF, Korevaar DA, Altman DG, Bruns DE, Gatsonis CA, Hooft L, et al. STARD 2015 guidelines for reporting diagnostic accuracy studies: explanation and elaboration. *BMJ Open* 2016;6:e012799
24. Shin JH, Baek JH, Chung J, Ha EJ, Kim JH, Lee YH, et al. Ultrasonography diagnosis and imaging-based management of thyroid nodules: revised Korean Society of Thyroid Radiology consensus statement and recommendations. *Korean J Radiol* 2016;17:370-395
25. Vassallo P, Werneck K, Roos N, Peters PE. Differentiation of benign from malignant superficial lymphadenopathy: the role of high-resolution US. *Radiology* 1992;183:215-220
26. Chung SR, Baek JH, Choi YJ, Sung TY, Song DE, Kim TY, et al. Diagnostic algorithm for metastatic lymph nodes of differentiated thyroid carcinoma. *Cancers (Basel)* 2021;13:1338

27. Lee JY, Yoo RE, Rhim JH, Lee KH, Choi KS, Hwang I, et al. Validation of ultrasound risk stratification systems for cervical lymph node metastasis in patients with thyroid cancer. *Cancers (Basel)* 2022;14:2106
28. Marchiori E, Hochegger B, Zanetti G. Lymph node calcifications. *J Bras Pneumol* 2018;44:83
29. Eisenkraft BL, Som PM. The spectrum of benign and malignant etiologies of cervical node calcification. *AJR Am J Roentgenol* 1999;172:1433-1437